arXiv:2112.01519v2 [cond-mat.str-el] 6 Jan 2022

Long-range entanglement from measuring symmetry-protected topological phases

Nathanan Tantivasadakarn,[1] Ryan Thorngren,[1,2,3] Ashvin Vishwanath,[1] and Ruben Verresen[1]

[1] *Department of Physics, Harvard University, Cambridge, MA 02138, USA*
[2] *Center for Mathematical Sciences and Applications, Harvard University, Cambridge, MA 02138, USA*
[3] *Department of Physics, Massachusetts Institute of Technology, Cambridge, MA 02139, US*

(Dated: January 7, 2022)

A fundamental distinction between many-body quantum states are those with short- and long-range entanglement (SRE and LRE). The latter cannot be created by finite-depth circuits, underscoring the nonlocal nature of Schrödinger cat states, topological order, and quantum criticality. Remarkably, examples are known where LRE is obtained by performing single-site measurements on SRE, such as the toric code from measuring a sublattice of a 2D cluster state. However, a systematic understanding of when and how measurements of SRE give rise to LRE is still lacking. Here we establish that LRE appears upon performing measurements on symmetry protected topological (SPT) phases—of which the cluster state is one example. For instance, we show how to implement the Kramers-Wannier transformation, by adding a cluster SPT to an input state followed by measurement. This transformation naturally relates states with SRE and LRE. An application is the realization of double-semion order when the input state is the $\mathbb{Z}_2$ Levin-Gu SPT. Similarly, the addition of fermionic SPTs and measurement leads to an implementation of the Jordan-Wigner transformation of a general state. More generally, we argue that a large class of SPT phases protected by $G \times H$ symmetry gives rise to anomalous LRE upon measuring G-charges. This introduces a new practical tool for using SPT phases as resources for creating LRE, and uncovers the classification result that all states related by sequentially gauging Abelian groups or by Jordan-Wigner transformation are in the same equivalence class, once we augment finite-depth circuits with single-site measurements. In particular, any topological or fracton order with a solvable finite gauge group can be obtained from a product state in this way.

CONTENTS

I. Introduction 1

II. Motivating examples 2

III. Kramers-Wannier as SPT 3
- A. Twisted gauge theory from measuring cluster + SPT phases 4
- B. Physically applying Kramers-Wannier to a gapless state 6
- C. Non-Abelian topological order from sequentially gauging Abelian groups 6

IV. Jordan-Wigner from measuring fermionic SPT phases 7

V. Generalizations 7
- A. LRE generation as stable property of SPT phase 8
  - 1. Plausibility argument 8
  - 2. Cat state from the spin-1 Heisenberg chain 8
- B. Measuring general SPT phases 9

VI. Outlook 10

Acknowledgments 11

References 11

A. Matrix product for the 1D cluster state and KW 15

B. More examples 15
- 1. Wen plaquette model 15
- 2. 3-Fermion Walker-Wang model 17
- 3. 2D Bosonization 18

C. Equality of long-range order for measurement outcomes in 1D 19

I. INTRODUCTION

Although quantum mechanics exhibits a dichotomy between unitary time-evolution and measurement, many-body quantum theory traditionally focuses on unitary aspects. Indeed, the classification of quantum phases of matter at zero temperature takes as its very definition that two states are in the same phase if and only if they can be connected by a unitary time-evolution in a finite time [1–7]. Any state in the same phase as a product state is said to exhibit short-range entanglement (SRE), whereas the other classes have long-range entanglement (LRE)[1]. Even restricting to gapped phases, the latter contains interesting cases such as intrinsic topological [8–13] and fracton order [14–20]. States with SRE can also

[1] Note, this definition of LRE includes some invertible phases like the Kitaev Majorana chain, since it cannot be connected to a product state by a finite-depth local unitary circuit.

be subdivided into distinct phases of matter if one imposes symmetry constraints on the aforementioned unitaries, giving rise to the notion of symmetry-protected topological (SPT) phases[2] [3, 4, 21–33].

Recently, there has been a growing interest in explicitly incorporating measurements into the study of many-body quantum states. For instance, a multitude of works have studied entanglement-reduction from measurements, giving rise to surprising new structures [34–50]. But there are also examples where measurements *increase* the entanglement. For example, it is known that performing single-site measurements on a subset of sites of a cluster state (with SRE) can produce a Greenberger-Horne-Zeilinger (GHZ) cat state [51], the toric code [52–54], and certain fracton codes via a layered construction [55, 56]. In fact, it has been remarked that all states realized by CSS stabilizer codes [57, 58] (i.e., stabilizers that are of the form $\prod_{\boldsymbol{i}\in\mathcal{S}} Z_{\boldsymbol{i}}$ or $\prod_{\boldsymbol{i}\in\mathcal{S}} X_{\boldsymbol{i}}$) can be obtained by measuring an appropriate cluster state [59].

The existence of these examples begs the question: what is the general framework for when, how and why one can create LRE from SRE states and single-site measurements? In this work, we argue that the essential fact in the above examples is that the cluster state is an SPT. This deeper understanding confers at least four advantages. First, in contrast to earlier studies, we argue that LRE states are obtained on measuring not just the fixed point wave-function of the SPT but any state within the same phase. Second, the origin of LRE under measurement is tied to a specific anomaly involving the symmetries—related to the anomaly living at the boundary of the original SPT phase—thereby constraining the nature of the resulting LRE. Third, this allows for the preparation of states that are not realized by stabilizer codes, such as topological order described by twisted gauge theories or non-Abelian fracton orders [60–69]. Fourth, we achieve a new perspective on Kramers-Wannier (KW) [18, 70–77] and Jordan-Wigner (JW) [78–86] transformations. Indeed, we show how these nonlocal transformations can be efficiently implemented in a finite time by adding SPT entanglers to arbitrary initial states[3] and subsequently performing single-site measurements. In a companion work [87], we explain how this general understanding can be utilized to prepare, e.g., $\mathbb{Z}_3$, S_3 and D_4 topological order in quantum devices such as Rydberg atom arrays.

This work is structured as follows. In Section II, we set the stage by reviewing some known examples, explaining how the 1D GHZ and 2D toric code states can be obtained by measuring particular cluster states. In Section III, we generalize this by reinterpreting the act of measuring cluster states as effectively implementing a KW transformation. To give illustrative examples, we explain how this allows one to transform the non-trivial $\mathbb{Z}_2$ SPT in 2D to the double-semion topological order, and to transform the 1D XY chain into two decoupled Ising transitions by using finite-depth circuits and single-site measurements. Moreover, we discuss how certain types of non-Abelian topological order can be obtained by sequential applications of this scheme. Section IV generalizes this to the fermionic case, where a similar procedure implements the JW transformation, illustrated by creating the Kitaev chain from a trivial spin chain. Section V broadens our scope further: first we argue that this procedure is a robust property of the SPT phase (which we exemplify by obtaining cat states via measuring the spin-1 Heisenberg chain), and second we argue that anomalous symmetries and LRE are generically obtained by measuring a broad class of SPT states (which we discuss in detail for the $\mathbb{Z}_2^3$ SPT in 2D). We conclude with future directions in Section VI.

II. MOTIVATING EXAMPLES

We begin by reviewing how measuring cluster states in 1D and 2D can produce GHZ states [51] and the toric code [52] respectively. Consider a 1D chain with $2N$ qubits. The cluster state $|\psi\rangle$ on this chain is the unique state that satisfies $Z_{n-1}X_nZ_{n+1}|\psi\rangle = |\psi\rangle$ for all n, where X, Y, Z denote the Pauli matrices. It can be prepared from the product state in the X-basis by applying Controlled-Z gates on all nearest neighboring qubits:

$$|\psi\rangle = \prod_n CZ_{n,n+1}|+\rangle^{\otimes 2N} =: U_{CZ}|+\rangle^{\otimes 2N}. \quad (1)$$

We will call the above unitary U_{CZ} the cluster state entangler. Now suppose we measure X on all odd sites, with outcomes $X_{2n+1} = (-1)^{s_{2n+1}}$. Since $Z_{2n-2}X_{2n-1}Z_{2n}$ commutes with the measurement, the state after the measurement $|\psi_{\text{out}}\rangle$ satisfies $Z_{2n-2}Z_{2n}|\psi_{\text{out}}\rangle = (-1)^{s_{2n-1}}|\psi_{\text{out}}\rangle$. On the other hand, the even stabilizers do not commute with the measurement; only their product $\prod_n Z_{2n-1}X_{2n}Z_{2n+1} = \prod_n X_{2n}$ commutes, implying $|\psi_{\text{out}}\rangle$ is $\mathbb{Z}_2$-symmetric. If all the $s_m = 0$, then $|\psi_{\text{out}}\rangle$ is thus the GHZ state on the even qubits:

$$|\text{GHZ}\rangle = \frac{1}{\sqrt{2}}\left(|\uparrow\uparrow\cdots\uparrow\rangle + |\downarrow\downarrow\cdots\downarrow\rangle\right). \quad (2)$$

Otherwise, it is the GHZ state up to single-site spin flips conditioned on the measurement outcomes: $|\text{GHZ}\rangle = \prod_{n=1}^N X_{2n}^{\sum_{m=1}^n s_{2m-1}}|\psi_{\text{out}}\rangle$. Thus, regardless of the outcome, $|\psi_{\text{out}}\rangle$ has long-range entanglement, as can for example be quantified by quantum Fisher information [88, 89] (see also Section V A 2).

In 2D, we can consider a cluster state on the vertices and edges of the square lattice [52]. The stabilizers of the

[2] Symmetry-broken states can also be regarded as SRE. However, for the purposes of the present work, we will consider their symmetry-preserving cat states, which exhibit LRE.

[3] This is equivalent to stacking SPT states on top of the initial state.

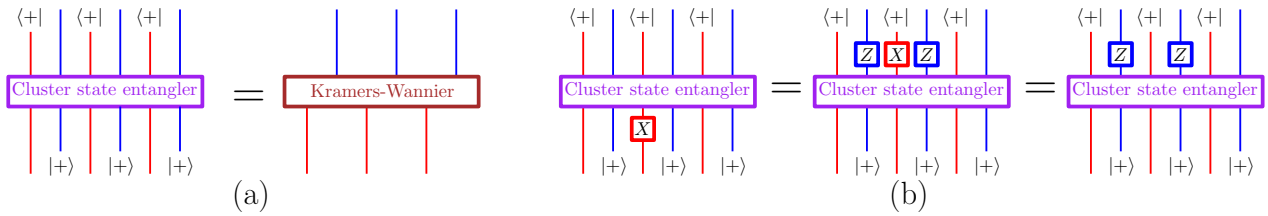

FIG. 1. **From cluster state entangler to Kramers-Wannier.** (a) The relation between the cluster state entangler and the Kramers-Wannier duality in arbitrary dimensions, with A legs drawn in red and B legs drawn in blue. Here the entangler is simply a product of controlled-Z on nearest-neighbor sites. (b) A proof of this equality at the level of operators where X on the red sites is interchanged with ZZ on the blue sites.

cluster state for each vertex and edge are $X_v \prod_{e\supset v} Z_e$ and $X_e \prod_{v\subset e} Z_v$ respectively, where $e \supset v$ and $v \subset e$ denotes edges e that contain the vertex v, and vertices v that are contained in e, respectively. Measuring X on all the edges will give a GHZ state on the vertices (up to spin flips that depend on measurement outcomes). On the other hand, measuring X on all the vertices gives a state of the toric code: we have the vertex term of the toric code, $\prod_{e\supset v} Z_e = \pm 1$ depending on the measurement outcome, and we have the plaquette operator $\prod_{e\subset p} X_e = 1$ coming from a product of for edge stabilizers around a plaquette, which commutes with the measurement. Note that while the topological order of this state is independent of the sign of the aforementioned stabilizers, one can always bring this to a state with $\prod_{e\supset v} Z_e = +1$ by applying string operators that pair up the vertices with $\prod_{e\supset v} Z_e = -1$.

III. KRAMERS-WANNIER AS SPT

We have seen that long-range entangled states can be obtained by performing single-site measurements on the cluster state. To explore a deeper reason for this, we will show how the cluster state secretly encodes the Kramers-Wannier (KW) transformation. For simplicity, we will first discuss the 1D case, where the KW transformation is defined as the map $X_n \to Z_n Z_{n+1}$ and $Z_{n-1}Z_n \to X_n$; although this preserves the locality of $\mathbb{Z}_2$-symmetric operators, it is a nonlocal mapping, relating SRE to LRE.

A first hint of the connection between the cluster state and the KW transformation is the fact that $Z_n Z_{n+2}$ and X_{n+1} act the same way on the cluster state. Even better, $X_{n+1}U_{CZ} = U_{CZ} Z_n X_{n+1} Z_{n+2}$, where U_{CZ} is the cluster entangler Eq. (1). Let us divide the sites into the odd and even sublattices, denoted A and B, respectively and define the states $|+\rangle_{A,B}$ on these subspaces. We find that the operator $\sigma := \langle +|_A U_{CZ} |+\rangle_B : \mathcal{H}_A \to \mathcal{H}_B$ gives the KW transformation. For example, we show that X_A is correctly mapped to $Z_B Z_B$, i.e., $\sigma X_A = Z_B Z_B \sigma$:

$$\begin{aligned} \langle +|_A U_{CZ} |+\rangle_B X_A &= \langle +|_A U_{CZ} X_A |+\rangle_B \\ &= \langle +|_A Z_B X_A Z_B U_{CZ} |+\rangle_B \\ &= \langle +|_A Z_B Z_B U_{CZ} |+\rangle_B \\ &= Z_B Z_B \langle +|_A U_{CZ} |+\rangle_B , \end{aligned} \tag{3}$$

and vice versa. This is depicted graphically in Fig. 1. Note that this works on any bipartite graph using a suitably generalized cluster state in any dimensions, in which case, the Z_B's that appear act on the B vertices adjacent to where X_A acts and vice versa.

This suggests a method to apply KW by measurement. We begin with a state in $\mathcal{H}_A$ and then introduce the ancillas $|+\rangle_B$. We then apply U_{CZ} to the combined system and measure the X spins on A. If the measurement outcomes are all $+$ spins, then we have exactly implemented the KW duality. Otherwise, we have instead implemented the closely related operator

$$M = \langle +|_A \left(\prod_{a\in A} Z^{s_a} \right) U_{CZ} |+\rangle_B = \sigma \prod_{a\in A} Z^{s_a} \tag{4}$$

where $s_a \in \{0,1\}$ are the measurement outcomes of site a. By pushing through the excess operators from the A sites to the B sites using σ, we can rewrite this as

$$M = \left(\prod_{b\in B} X^{s_b} \right) \langle +|_A U_{CZ} |+\rangle_B = \left(\prod_{b\in B} X^{s_b} \right) \sigma, \tag{5}$$

where the s_b are functions of the s_a which depend on the graph. For example, in 1D, where A and B are the odd and even sublattices of the chain respectively, we have $s_b = \sum_{1<a<b} s_a$. Thus, we see that further applying $\left(\prod_{b\in B} X^{s_b}\right)$ restores the exact KW mapping σ. See Fig. 2.

This explains why the measured 1D cluster state has long-range order—it produces the KW dual of the trivial state $|+\rangle_A$, which is a GHZ state. Likewise in 2D we obtain the KW dual of the trivial state which is a toric code state[4].

[4] We note that as a by-product, we obtain explicit tensor network

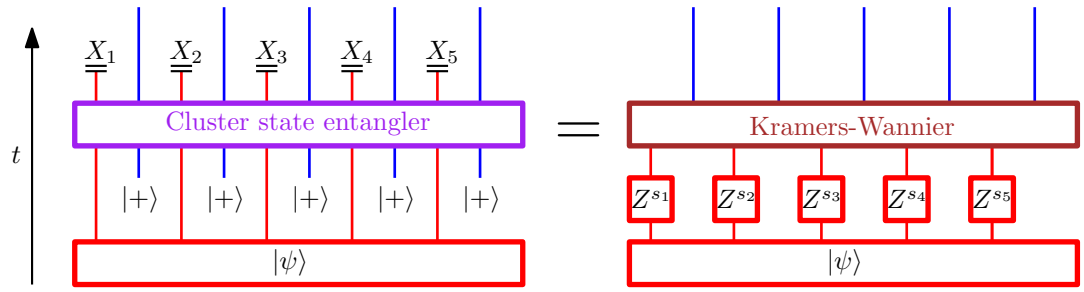

FIG. 2. **Kramers-Wannier from finite-depth circuit and measurements.** Using the cluster state entangler to implement Kramers-Wannier duality by measurement. The final state depends on $s_n = 0, 1$ corresponding to measurement outcomes $X_n = 1, -1$ respectively, which we can express as a product $\prod_n Z^{s_n}$ applied to $|\psi\rangle$ before KW transformation. These operators can be pushed through the KW transformation to obtain a product of X operators on the B sublattice (blue). Hence, by acting with this product on the post-measurement state, one can obtain the KW transformation of $|\psi\rangle$ without post-selection.

We will later argue that the long-range order holds for any state in the same SPT phase as the cluster state. Indeed, this can be seen by symmetry fractionalization for the two $\mathbb{Z}_2$ symmetries $\prod_{a\in A} X_a$ and $\prod_{b\in B} X_b$ (acting on the odd and even sublattices, respectively) protecting the SPT phase. If we act on any state $|\psi\rangle$ in the same SPT phase by the $\mathbb{Z}_2^A$ symmetry in a region $\mathcal{R}$, it will reduce to some $\mathbb{Z}_2^B$ charged operators at the boundary of the region: $\prod_{a\in\mathcal{R}} X_a |\psi\rangle = \mathcal{O}_L \mathcal{O}_R |\psi\rangle$, where $\mathcal{O}$ is some operator with finite support situated at the left and right boundaries of $\mathcal{R}$ that anticommutes with $\mathbb{Z}_2^B$. Intuitively this means that $|\psi\rangle$ has the KW property, exchanging order operators and disorder operators, at long distances. See Section V A 1.

In higher dimensions, the cluster state is an SPT for higher form or subsystem symmetries which depend on the lattice. For example, if A and B are sites at the vertices and edges of the square lattice, then we have symmetries $\prod_{a\in A} X_a$ and $\prod_{b\in\gamma\subset B} X_b$, where we have a symmetry for each closed curve γ drawn along the edges of the direct lattice. The KW so constructed is the duality between the Ising model and Ising gauge theory in 2+1D.

A summary of examples that arise from the KW transformation of various symmetries is given in Table I

A. Twisted gauge theory from measuring cluster + SPT phases

As a first application, we discuss what happens when we apply this procedure to other states on the A sublattice, such as an SPT. As in Fig. 2, we add $|+\rangle_B$ ancillas, couple A and B with the cluster state entangler, and then perform measurements on the A sublattice. The result of this procedure is equivalent to gauging the SPT phase[5].

To illustrate this procedure, we discuss how beginning with the A sublattice in the pure $\mathbb{Z}_2$ or "Levin-Gu" SPT state $|\psi\rangle$ [31] we obtain the double semion topological order [12] after entangling and measuring. The Levin-Gu SPT is defined on the vertices of the triangular lattice (A) and is an eigenstate of the following (non-Pauli) stabilizers:

$$X_v \prod_{\langle vuu'\rangle} e^{\frac{\pi i}{4} Z_u Z_{u'}} = \tag{6}$$

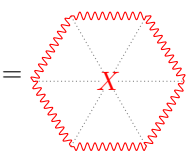

where $\langle vuu'\rangle$ are the six triangles around v, and visually the wavy lines denote $e^{\frac{\pi i}{4} Z_u Z_{u'}}$ between vertices u and u'. Note, this stabilizer is not simply a product of Pauli operators. Let us also stress that since this an SPT phase, it is possible to prepare this state by a finite-depth circuit[6]. Following our procedure, we add the B sublattice consisting of edges of the triangular lattice, supporting a product with the trivial stabilizer

$$X_e = \tag{7}$$

Next, we couple the two with the cluster state entangler.

representations of these states. This offers an alternative derivation of the 3D toric and fracton code projected entangled pair states (PEPS) [90, 91] obtained in Refs. [92, 93].

[5] Alternatively, by viewing the SPT and the cluster state as a single state, performing the measurement on this combined SPT can be thought of as a different way of performing the KW duality on the product state. This choice of adding an extra SPT before gauging is also known discrete torsion[94], or defectification classes [95] in the literature.

[6] The unitary that creates the Levin-Gu SPT is given by $e^{\frac{i\pi}{8}(\sum_{\Delta_{uvw}} Z_u Z_v Z_w - 2\sum_v Z_v)}$ where Δ_{uvw} denotes all triangles.

D	A Symmetry	B symmetry	SPT	Product state maps to	See
1	$\mathbb{Z}_2$	$\mathbb{Z}_2$	AB	GHZ	II
1	$\mathbb{Z}_2$	$\mathbb{Z}_2^F$	ηA	Kitaev chain	IV
2	$\mathbb{Z}_2$	$\mathbb{Z}_2[1]$	AB	Toric Code	II
2	$\mathbb{Z}_2$	$\mathbb{Z}_2[1]$	$A^3 + AB$	Double Semion	III A
2	$\mathbb{Z}_2$ (2-foliated line)	$\mathbb{Z}_2$ (2-foliated line)	"$A^2 + AB$" (strong) SSPT	Wen plaquette	B 1
3	$\mathbb{Z}_2[1]^2$	$\mathbb{Z}_2[1]^2$	$A_1^2 + A_2^2 + A_1A_2 + A_1B_2 + A_2B_1$	3-Fermion Walker-Wang	B 2
3	$\mathbb{Z}_2$ (3-foliated planar)	$\mathbb{Z}_2$ (dual subsystem)	"AB" SSPT	X-cube	[87]
3	$\mathbb{Z}_2$ (fractal)	$\mathbb{Z}_2$ (dual fractal)	"AB" fractal SSPT	Sierpinski fractal spin liquid	[87]

TABLE I. Examples of states obtained by measuring SPTs. After evolving the product state with the corresponding SPT entangler, the A sublattice is measured, effectively performing a KW or JW transformation to the product state. All SPTs listed except those that create the Kitaev chain and double semion model are cluster states. D is the space dimensions, $\mathbb{Z}_2[1]$ denotes a $\mathbb{Z}_2$ 1-form symmetry, and A, B denote gauge fields defined for the A and B symmetries, respectively. See Sec. V B for examples which go beyond this framework.

This results in stabilizers

$$X_v \prod_{\langle vuu'\rangle} e^{\frac{\pi i}{4} Z_u Z_{u'}} \prod_{e\supset v} Z_e = \tag{8}$$

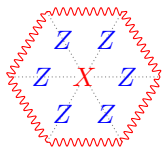

$$X_e \prod_{v\subset e} Z_v = \tag{9}$$

Before we perform the measurements on all A sites (the vertices of the triangular lattice), we note that the vertex stabilizer does not commute with the measurement. It would thus not directly give us a useful condition on the post-measurement state. However, using the fact that $Z_u Z_{u'} |\psi\rangle = X_{(uu')} |\psi\rangle$, where (uu') is the edge with u and u' as endpoints, the following is an equally valid set of stabilizers of $|\psi\rangle$

$$X_v \prod_{\langle vuu'\rangle} R_{(uu')} \prod_{e\supset v} Z_e = \tag{10}$$

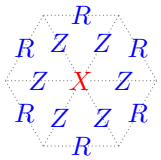

$$X_e \prod_{v\subset e} Z_v = \tag{11}$$

where $R_e = e^{\frac{\pi i}{4} X_e}$. The vertex stabilizers now commute with the measurement. However, the stabilizers in Eq. (10) do not commute for adjacent vertices. This however is cured by restricting to the subspace:

$$\prod_{e\subset\Delta} X_e = \tag{12}$$

$= 1.$

We can therefore circumvent having non-commuting stabilizers by attaching

$$O_{vuu'} = \frac{1 + X_{(vu)} X_{(vu')} X_{(uu')}}{2} = \tag{13}$$

which is a projector into this subspace into each triangle. So finally, $|\psi\rangle$ is identified as the unique state that has eigenvalue $+1$ under the following operators

$$X_v \prod_{\langle vuu'\rangle} \left(R_{(uu')} O_{vuu'}\right) \prod_{e\supset v} Z_e = \tag{14}$$

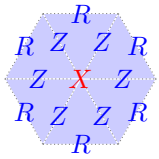

$$X_e \prod_{v\subset e} Z_v = \tag{15}$$

Performing the measurement with outcomes $X_v = (-1)^{s_v}$, the post-measurement state is the unique state that has eigenvalue $+1$ under the operators:

$$(-1)^{s_v} \prod_{\langle vuu'\rangle} \left(R_{(uu')} O_{vuu'}\right) \prod_{e\supset v} Z_e = (-1)^{s_v} \tag{16}$$

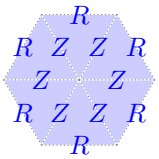

$$\prod_{e\subset\Delta} X_e = \tag{17}$$

This is the ground state of the double semion model [31] up to single site X-rotations on edges that pair up the vertices where $s_v = 1$ to remove the signs, and swapping X_e with Z_e to match the choice in Ref. [31].

Our implementation of gauging via combining measurements with a cluster state entangler (including $\mathbb{Z}_n$ generalizations) implies that we can produce all twisted quantum double models of finite Abelian gauge group via stacking general SPTs prior to measuring—which can be prepared by finite-depth circuits [27]. Note that this already contains certain non-Abelian phases, e.g., D_4 topological order arises upon gauging the $\mathbb{Z}_2^3$ symmetry of an SPT phase with type-III cocycle [96, 97]. (For obtaining non-Abelian topological order associated to any solvable

group, see Section III C.) Similarly, our procedure allows for the creation of twisted fracton phases by gauging 3D subsystem SPT phases [65, 83, 84, 98, 99]. Thus a much wider class of states can be obtained from local unitary circuits and LOCC (local operations and classical communications) [54] than previously established.

B. Physically applying Kramers-Wannier to a gapless state

Here, we discuss an example where the input state $|\psi\rangle$ in Fig. 2 itself has long-range entanglement. In particular, we focus on a well-known example of how the XY chain—an example of a gapless state—can be transformed into two decoupled critical Ising chains by gauging particle-hole symmetry[7]. Here, we achieve this gauging by using a finite-depth circuit and single-site measurements.

We place the XY chain on the odd sites (A) and initialize with $|+\rangle$ states on the even sites (B). The aforementioned state can be considered the ground state of the following Hamiltonian

$$H = \sum_n X_{2n-1}X_{2n+1} + Y_{2n-1}Y_{2n+1} - X_{2n} \tag{18}$$

We couple the even and odd sites with the cluster state entangler $U = \prod_n CZ_{n,n+1}$, resulting in

$$\begin{aligned} UHU^\dagger = &\sum_n Z_{2n-2}(X_{2n-1}X_{2n+1} + Y_{2n-1}Y_{2n+1})Z_{2n+2} \\ &- Z_{2n-1}X_{2n}Z_{2n+1} \end{aligned} \tag{19}$$

Note that since $Z_{2n-1}X_{2n}Z_{2n+1}$ is an integral of motion, the following Hamiltonian also has the same wavefunction as its ground state

$$\sum_n Z_{2n-2}(X_{2n-1}X_{2n+1} - X_{2n})Z_{2n+2} - Z_{2n-1}X_{2n}Z_{2n+1} \tag{20}$$

Now we perform a measurement on the odd sites with measurement outcomes $X = (-1)^s$, the state after the measurement is the ground state of the Hamiltonian

$$\sum_n (-1)^{s_{2n-1}+s_{2n+1}} Z_{2n-2}Z_{2n+2} - Z_{2n-2}X_{2n}Z_{2n+2} \tag{21}$$

with integral of motion $\prod_n X_{2n}$ serving as a global $\mathbb{Z}_2$ symmetry. After appropriate spin flips to remove the signs, and the circuit $\prod_n CZ_{2n,2n+2}$, the Hamiltonian reads

$$\sum_n Z_{2n-2}Z_{2n+2} - X_{2n} \tag{22}$$

which describes two decoupled critical Ising chains. We thus confirm that we have physically implemented the KW transform on a gapless state.

C. Non-Abelian topological order from sequentially gauging Abelian groups

Beyond cyclic groups $\mathbb{Z}_n$, cluster states and the corresponding KW dualities have been generalized to arbitrary finite groups [101–103], giving the potential to gauge non-Abelian groups by unitaries and measurement. However, unlike the Abelian case, which produces Abelian anyons depending on the measurement outcome, gauging non-Abelian groups can produce non-Abelian anyons that can only be paired up using linear depth string operators[8]. The intuition for this is that the string operators for moving such anyons consist of noncommuting operators which hence cannot be applied all at once[9].

Our implementation of the KW duality avoids this issue by a sequence of circuits and measurements, which can be interpreted as sequentially gauging Abelian groups. In such a method, the measurement outcomes in all intermediate states correspond to Abelian anyons, which can all be paired up in finite depth. In this way, all gauge theories whose gauge group is solvable (i.e., obtained by extending finite Abelian groups) can be constructed efficiently in this manner. For example, the S_3 quantum double can be obtained by gauging a $\mathbb{Z}_3$ symmetry (i.e., measuring a $\mathbb{Z}_3$ cluster state), which prepares a $\mathbb{Z}_3$ toric code, followed by gauging the charge conjugation symmetry that permutes anyons $e \leftrightarrow e^2$ and $m \leftrightarrow m^2$. We note that since S_3 is not nilpotent, it can be used for universal quantum computation [104]. As a second example, the D_4 topological order can be obtained by first preparing the 2D color code, and gauging the Hadamard symmetry. In our companion paper we provide explicit finite-depth qubit-based circuits for these two examples [87].

We note that sequentially gauging Abelian groups can also give rise to states beyond quantum doubles. For instance, the doubled Ising anyon theory can be obtained by gauging the $e \leftrightarrow m$ symmetry of $\mathbb{Z}_2$ topological order [95]. Such a Kramers-Wannier transformation (implemented using our finite-depth circuit and single-site

[7] Field theoretically, this maps the compact boson to two copies of the Ising CFT [100].

[8] We thank David T. Stephen for pointing out this subtlety.

[9] We note one potential loophole. If the group is nilpotent, two non-Abelian anyons can be annihilated by first nucleating a whole density of pairs of anyons of the same type along a path connecting the two anyons and subsequently fusing them all at once. This potentially leaves a density of residual anyons all along the path, but the nilpotent sequence ensures that by repeating this process, we obtain simpler and simpler anyons—eventually leading to Abelian anyons which can be efficiently removed. Unfortunately, the known ways of using non-Abelian states for universal quantum computation rely on the group being not nilpotent [104].

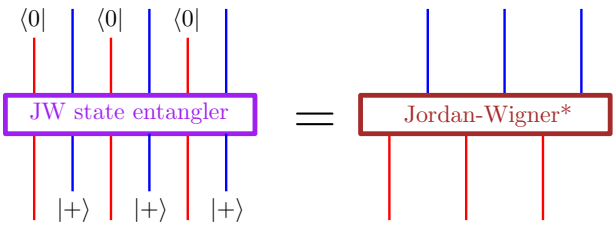

FIG. 3. **Jordan-Wigner from finite-depth circuit and measurements.** Entangling fermionic (red) and bosonic (blue) degrees of freedom and its relation to the JW transformation. Here $\langle 0|$ corresponds to contracting with the empty state of fermions. We use Jordan-Wigner* to emphasize that this transformation differs from the usual JW by an additional KW transformation. Similar to Fig. 2, this can be utilized to implement the JW transformation via measurements (see main text).

measurements) can indeed be performed since it is known that the $\mathbb{Z}_2$ symmetry can be made on-site (for explicit models, see Refs. [105, 106]). By definition, this state can be connected to any other state with $\mathbb{Z}_2$ topological order through a finite-depth circuit, and we have already described how, e.g., the usual toric code can be obtained from the product state.

IV. JORDAN-WIGNER FROM MEASURING FERMIONIC SPT PHASES

Analogous to the KW transformation, the Jordan-Wigner (JW) is a nonlocal transformation which maps between fermionic and bosonic degrees of freedom [78, 79]. Similar to KW, here we can prepare and entangle bosonic and fermionic degrees of freedom as shown in Fig. 3. We can then perform either bosonization of an arbitrary input fermionic state by measuring the parity of all fermions, or fermionization of an arbitrary input bosonic state by measuring X on all the spins after the entangling step.

Let us demonstrate this explicitly by preparing the Kitaev Majorana chain, which cannot be done in finite time with only unitary evolution [6]. We start with N qubits on odd sites initialized in the $|+\rangle$ state and N fermions on even sites initialized in the empty state $P = -i\gamma\gamma' = 1$ where $\gamma = c + c^\dagger$ and $\gamma' = -i(c - c^\dagger)$ are Majorana operators. Furthermore, we define the hopping operator $S_{2n} = i\gamma'_{2n-2}\gamma_{2n}$, which hops a fermion from site $2n-2$ to $2n$. We create a $\mathbb{Z}_2 \times \mathbb{Z}_2^F$ SPT [107–110] with the following circuit

$$U = \prod_{n=1}^{N} CS_{2n-1,2n} \tag{23}$$

where the operator

$$CS_{2n-1,2n} = |\uparrow\rangle\langle\uparrow|_{2n-1} + |\downarrow\rangle\langle\downarrow|_{2n-1} S_{2n} \tag{24}$$

is a hopping operator controlled by the qubit at $2n-1$. That is, a fermion is hopped if the spin at site $2n-1$ is down. We also remark that because all gates mutually commute, it can be implemented as a finite depth circuit. The resulting SPT is given by the stabilizers

$$UX_{2n-1}U^\dagger = i\gamma'_{2n-2}X_{2n-1}\gamma_{2n}, \tag{25}$$

$$UP_{2n}U^\dagger = Z_{2n-1}P_{2n}Z_{2n+1}. \tag{26}$$

Now, we measure the all the spins with outcomes $X_{2n-1} = (-1)^{s_{2n-1}}$. The stabilizers of the measured state are $(-1)^{s_{2n-1}}\gamma'_{2n-2}\gamma_{2n}$ and $\prod_n Z_{2n-1}P_{2n}Z_{2n+1} = \prod_n P_{2n}$, which after applying $\prod_{n=1}^{N} P_{2n}^{\sum_{m=1}^{n} s_{2m-1}}$, gives the ground state of the Kitaev chain. We note that alternatively, starting with the SPT, measuring the parity of all the fermions gives the GHZ state.

We can even extend this procedure to arbitrary dimensions. The generalization of Jordan-Wigner has been explored in a number of works including [80–86, 111**?** , 112]. From this we can construct a particular state of fermions and spins which conserves fermion parity and a higher form $\mathbb{Z}_2$ symmetry such that one can perform either bosonization, by measuring the parity of each fermion, or fermionization, by measuring the spins in the X-basis. In Appendix B 3, we give an explicit way of preparing the JW state.

Similarly to the KW, we can now apply JW to arbitrary states by measurements. For example, we can consider preparing the fermions in a 2+1D topological $p+ip$ superconducting state with chiral Majorana edge modes. After coupling to the JW state and measuring fermion parity, the remaining spins will describe a chiral Ising topological order. Similarly, coupling ν stacks of $p+ip$ superconductors to the SPT and performing the measurement can realize the topological orders in Kitaev's 16-fold way [13].

V. GENERALIZATIONS

Thus far we have focused on two illustrative cases, where measuring sublattices of the cluster and JW states leads to LRE. In this last section, we generalize this in two directions. First, we make the case that the ability to produce LRE from measurement is indeed a property of the whole SPT *phase*, being robust to tuning away from a fixed-point limit. Second, we show that LRE is naturally obtained by measuring a broad class of SPT phases, of which the cluster and JW states are but two examples.

A. LRE generation as stable property of SPT phase

1. Plausibility argument

Let us first consider the 1D cluster SPT phase and ask whether one obtains a cat state upon measuring one of the sublattices starting with an arbitrary state in this phase. We present an intuitive argument, which holds away from the fixed-point limit. A key property of the cluster SPT phase in 1D is that it generically has long-range order for the following string operator [113]:

$$\lim_{|n-m|\to\infty} \langle Z_{2m}\mathcal{S}_{2m,2n}Z_{2n}\rangle = C \neq 0, \tag{27}$$

where $\mathcal{S}_{2m,2n} := X_{2m+1}X_{2m+3}\cdots X_{2n-1}$ is a string operator consisting of the $\mathbb{Z}_2$ symmetry of the odd sites. The SPT invariant [114] is encoded in the fact that the string operator for one of the $\mathbb{Z}_2$ symmetries only has long-range order if one includes an endpoint operator which is charged under the *other* $\mathbb{Z}_2$ symmetry. Indeed, in the non-trivial SPT phase, one finds that the undressed string does not have long-range order:

$$\lim_{|n-m|\to\infty} \langle \mathcal{S}_{2m,2n}\rangle = 0. \tag{28}$$

Let us now measure the odd sites in the X-basis. Since measurements commute, we can imagine that our very first step is to measure the whole string $\mathcal{S}_{2m,2n}$, for a fixed choice of m and n. Note that Eq. (28) tells us that if we choose n and m far enough apart, then $\langle \mathcal{S}_{2m,2n}\rangle \approx 0$. Hence, both measurement outcomes $\mathcal{S}_{2m,2n} = \pm 1 = (-1)^s$ are equally likely. The two possible post-measurement states can thus be written as:

$$|\psi_s\rangle = \frac{1}{\sqrt{2}}\left(1 + (-1)^s \mathcal{S}_{2m,2n}\right)|\psi\rangle. \tag{29}$$

Plugging $|\psi\rangle = \frac{1}{\sqrt{2}}\left(|\psi_0\rangle + |\psi_1\rangle\right)$ into Eq. (27), we obtain:

$$\langle\psi_0|Z_{2m}Z_{2n}|\psi_0\rangle - \langle\psi_1|Z_{2m}Z_{2n}|\psi_1\rangle = 2C. \tag{30}$$

Moreover, using the dual string operator, one can prove that $\langle\psi_0|Z_{2m}Z_{2n}|\psi_0\rangle = -\langle\psi_1|Z_{2m}Z_{2n}|\psi_1\rangle$ (see Appendix C), such that for either measurement outcome we have:

$$|\langle\psi_i|Z_{2m}Z_{2n}|\psi_i\rangle| = |C| \neq 0. \tag{31}$$

We thus find that measuring the string leads to long-range cat-state-like entanglement between the two endpoints! This result is consistent with the notion of SPT entanglement explored in Ref. [115].

The above argument can be extended to higher dimensions. For instance, let us revisit the 2D case mentioned in Section II: the square lattice with spins on the vertices (A sublattice) and bonds (B sublattice). The cluster state on this lattice is an SPT phase protected by a global $\mathbb{Z}_2$ symmetry $U^A = \prod_{a\in A} X_a$, as well as a "1-form symmetry", $U^B_\gamma = \prod_{b\in\gamma\subset B} X_b$, meaning a symmetry defined for each closed curve γ on the bonds of the square lattice [97, 116, 117].

In the SPT phase, we have long-range order for the membrane operator $S_{\partial R}\prod_{a\in A\cap R} X_a$ where R is some region and $S_{\partial R}$ is a string operator on the boundary which "braids" with U^B_γ, meaning $U^B_\gamma S_{\gamma'}(U^B_\gamma)^\dagger = S_{\gamma'}(-1)^{\gamma\cap\gamma'}$, where the exponent is the number of intersection points between the curves γ and γ'. For the fixed point cluster state, $S_{\gamma'} = \prod_{b\in\gamma'} Z_b$.

Upon measuring the membrane, we are left with long-range order for S_γ (see Fig. 5). This serves as an order parameter for spontaneously breaking the 1-form symmetry, thereby implying topological order. In fact, this point of view naturally generalizes to other SPT phases, as we will discuss in Section V B.

However, while the above is intuitive and encouraging, it is does not strictly prove that the LRE persists upon measuring all the sites. In particular, in the 1D case, we have thus far only measured $\mathcal{S}_{2m,2n}$, and not yet all odd sites. There may be no guarantee that the long-range order in Eq. (31) persists after performing the other measurements[10]. We do expect this to generically hold (i.e., with probability one) if it indeed holds in the fixed-point limit—which we have already established in the case of the cluster and JW states. To check that it does indeed persist in an example, we now turn to a numerical exploration of a generic point in this SPT phase.

2. Cat state from the spin-1 Heisenberg chain

While it is known that performing measurements on the 1D cluster state can prepare a cat state [51], our claim is that this is a generic feature of a $\mathbb{Z}_2\times\mathbb{Z}_2$ SPT phase in 1D. To emphasize the generality of this claim, we can even consider a different incarnation of it as the Haldane SPT phase of the spin-1 Heisenberg chain, with just nearest-neighbor antiferromagnetic coupling:

$$H = \sum_n \boldsymbol{S}_n \cdot \boldsymbol{S}_{n+1}. \tag{32}$$

This spin chain is known to be gapped [118], forming a non-trivial SPT phase for the $\mathbb{Z}_2\times\mathbb{Z}_2$ group of π-rotations generated by $R^\gamma = \prod_n e^{i\pi S^\gamma_n}$ with $\gamma = x, y, z$ [21, 119–121].

By our general proposal, we expect that measuring, say, the R^z charge for every site, should result in a cat state for the remaining $\mathbb{Z}_2$ symmetry. An interesting difference from the cluster chain is that now the symmetries do not act on distinct sites. We must thus measure $R^z_n = e^{i\pi S^z_n}$ on *every single* site. Effectively, this comes

[10] In fact, in the argument we gave for the 2D case, the unitary string operator U might have overlap with the very sites that we are measuring.

down to measuring whether $(S_n^z)^2$ is 0 or 1. For the first outcome, the site has no degree of freedom left, whereas for the latter, we still have a remaining qubit ($S_n^z = \pm 1$) which is toggled by R^x. Hence, with the exception of the probability zero case of only finitely many $(S_n^z)^2 = 1$, we expect a cat state for the remaining chain of qubits.

To test this prediction, we numerically obtain the ground state of Eq. (32) using the density matrix renormalization group (DMRG) [122–124] for a variable system size L with periodic boundary conditions. We then project each site into $(S_n^z)^2 = 0$ with probability 1/3 or $(S_n^z)^2 = 1$ with probability 2/3. As a robust way of detecting whether the resulting state is a cat state, we calculate the Fisher information, which in this case is simply the variance of the total (staggered) magnetization:

$$F = \left\langle \left(\sum_{n=1}^{L} (-1)^n S_n^z \right)^2 \right\rangle - \left\langle \sum_{n=1}^{L} (-1)^n S_n^z \right\rangle^2 . \quad (33)$$

This Fisher information is a quantitative measure for the use of the state for quantum metrology purposes [88, 89]. While SRE states obey a scaling $F \sim L$, only nonlocal cat states have $F \sim L^2$. Our numerical results[11] are shown in Fig. 4. While the original ground state has $F \sim L$, we find that the post-measurement state indeed has $F \sim L^2$, confirming that it is a cat state. In addition, it is interesting to see that $F(L)$ varies relatively continuously with L, despite each system size having a completely random measurement outcome (each red dot is computed for only a single measurement shot).

The above emergence of a cat state can actually be linked to the original interpretation of the Haldane SPT phase. Indeed, when the topological string order parameter was first introduced in 1989 [120], it was designed to pick up the 'hidden symmetry-breaking' of the state, where it was observed that if one imagines removing all $S_n^z = 0$ states, then the remaining $S_n^z = \pm 1$ states form long-range Néel order. Since the $S_n^z = 0$ states are there and have quantum fluctuations, they disorder this local order (which can now only be picked up with a string order parameter). Our above procedure can be interpreted as making this hidden order manifest: the measurement pins the location of $S_n^z = 0$, preventing them from disordering the Néel state.

B. Measuring general SPT phases

Here we discuss how LRE arises upon measuring SPT states beyond the cluster or JW states. As a natural starting point, we consider one of the simplest SPT phases (beyond 1D) which has more than single cyclic group—such that it is meaningful to measure one symmetry and preserve the other. Let us thus consider the $\mathbb{Z}_2^3$ "cubic" SPT in 2+1D. One model for this phase [97, 125] is given by placing spins on the sites of a triangular lattice, with each $\mathbb{Z}_2$ acting as $\prod_{j\in A,B,C} X_j$ on each of three triangular sublattices A, B, C. For each site j there is a stabilizer given by $S_j = X_j \prod_{\langle jqq'\rangle} CZ_{q,q'}$ where the product is over triangles $\langle jqq'\rangle$ with vertices j, q, q'. When we measure X_j on the A sublattice, we are left with a state on a honeycomb sublattice with $\prod_{\langle jqq'\rangle} CZ_{q,q'} = (-1)^{s_j}$ around each hexagon, for some fixed signs (determined by our measurement outcome s_j).

The loop operators $\prod_\gamma CZ_{\gamma_i,\gamma_j}$ along a closed path γ of vertices can be considered as a $\mathbb{Z}_2$ 1-form symmetry of this state. Note that this acts as the cluster SPT entangler for $\mathbb{Z}_2^{B,C}$ along γ. This implies there is a mixed anomaly and therefore the resulting state obtained from measurement cannot be trivially gapped. Note that this anomaly can be realized on the boundary of a lattice model of a 3D SPT protected by $\mathbb{Z}_2^2 \times \mathbb{Z}_2[1]$ studied in Ref. [97].

We believe that a similar conclusion holds generally when we measure SPT states, at least when the corresponding topological term is linear in the gauge field associated with the measured charge. That is, suppose we have an Abelian global symmetry $G \times H$ and an SPT with associated cohomology class $AF(B) \in H^{d+1}(G \times H, U(1))$, where d is the dimension of space. We think of this as a topological term where A and B are the gauge fields of G and H, respectively, and $F(B) \in H^d(H, G^\star)$ describes a topological G current made from B where $G^\star = \mathrm{Hom}(G, U(1))$. Physically, such SPTs can be con-

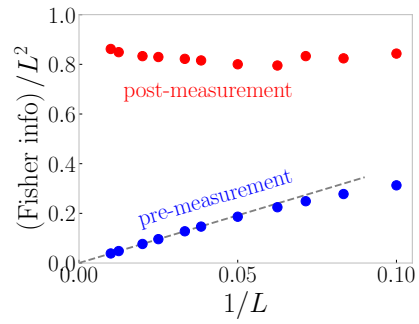

FIG. 4. **Cat state from measuring the Haldane SPT phase.** We consider the ground state of the spin-1 Heisenberg chain, which is in a non-trivial SPT phase for the $\mathbb{Z}_2 \times \mathbb{Z}_2$ symmetry of π-rotations. In accordance with its short-range entanglement, we find that the Fisher information scales linearly with system size (blue dots). In contrast, if we measure the $R_n^z = e^{i\pi S_n^z}$-charge on every site, the remaining state has Fisher information $F \sim L^2$ (red dots), signaling long-range entanglement in the post-meaurement state (here we have chosen different random measurement outcomes for each L). This confirms that measuring one $\mathbb{Z}_2$ symmetry of the Haldane SPT phase creates a cat state for the remaining $\mathbb{Z}_2$ symmetry, even if one is not at a fine-tuned fixed-point limit.

[11] We went up to system sizes of $L = 100$, where we found that $\chi \approx 500$ was sufficient to guarantee convergence of the Fisher information.

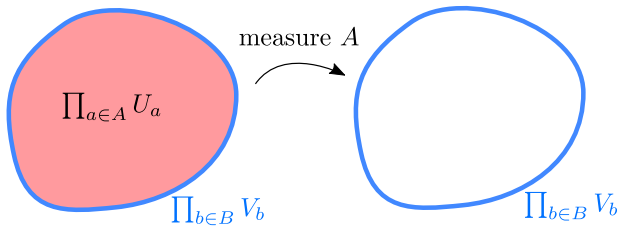

FIG. 5. **Anomalous symmetry from measuring an SPT phase.** In an SPT phase, applying the symmetry in a region is equivalent to applying a unitary operator just near the boundary of that region; equivalently, the membrane operator has long-range order if we include the appropriate unitary operator along its boundary. In the $G \times H$ SPT fixed point models of the linear form $AF(B)$, G acts only on the A sublattice and the boundary operator acts only on the B sublattice. If we then measure the spins of the A sublattice, this boundary operator remains as a symmetry, now locally defined along the boundary. Because the boundary is codimension 1, this defines a G 1-form symmetry. By virtue of the original state being a non-trival SPT phase, we find that this operator has a mixed anomaly with H, implying that the post-measurement state cannot be short-range entangled.

structed by decorating G-domain walls with H SPTs [126].

In this case, there is a fixed point model with two sets of degrees of freedom, one with G acting and the other with H acting. If we then measure the G charges, we essentially project out the topological current $F(B)$, analogous to the CZ ring terms above. We will also get a 1-form symmetry, the remnant of the G symmetry action, by symmetry fractionalization—applying the G symmetry in a region is equivalent to acting on the boundary of that region, and in this special model, it is equivalent to acting on only the H degrees of freedom on the boundary of the region, see Fig. 5.

In addition to the above lattice perspective, we can also interpret it field-theoretically. Applying the symmetry in a region R can be viewed as creating a G gauge field A Poincaré dual to R. Meanwhile, dA is dual to ∂R. After measuring, when the boundary becomes a free operator, we should replace dA with an arbitrary G-valued 2-form $\tilde{A}$. So by taking the differential of the SPT class, we now find the *anomaly* $\tilde{A}F(B) \in H^{d+2}(G[1] \times H, U(1))$ for the G 1-form (denoted $G[1]$ for the degree shift) and the H 0-form symmetry in the measured system. The cubic SPT anomaly we discussed above matches this with $G = \mathbb{Z}_2$, $H = \mathbb{Z}_2^2$, $A = A_1$, $B = (A_2, A_3)$, and $F(B) = \frac{1}{2}A_2A_3$. We conjecture that the existence of the 1-form symmetry and this anomaly holds for all states in this SPT class, not just the special fixed point ones which factorize. We therefore expect all these states to be long-range entangled.

When the SPT class is not linear in A, we will not be able to fractionalize the G symmetry so that the boundary operator commutes with the G charges [33]. However, if it is the form $F_1(A)F_2(B)$, $F_1 \in H^j(G, K)$, $F_2 \in H^{d+1-j}(G, K^*)$, for some Abelian group K, then there will be a codimension $j+1$ defect Poincaré dual to $dF_1(A)$ which can factorize, defining a $j+1$-form symmetry in a fixed point model. The anomaly will be $CF_2(B) \in H^{d+2}(K[j+1] \times H, U(1))$. This occurs with the cubic SPT when we measure both $\mathbb{Z}_2^A$ and $\mathbb{Z}_2^B$, yielding an anomaly $\frac{1}{2}CA_3$ for a $\mathbb{Z}_2$ 2-form symmetry associated with C.

VI. OUTLOOK

In this work we have presented a general framework for which performing measurements of short-range entangled states produce long-range entanglement. We have given some intuitive arguments that this is a stable property of the SPT phase. It would be very interesting to tighten these up, perhaps by constructing the anomalous symmetry of Sec. V B away from fixed point states. We would also like to determine the nature of the long-range entangled states which appear.

We have also described how non-local transformations including Kramers-Wannier and Jordan-Wigner arise from coupling an arbitrary state with a symmetry to a cluster-like SPT and performing measurements. It would be interesting to see whether other SPTs define useful transformations this way. If so, what family of MPOs do they define?

Sequential applications of our procedure even lead to non-Abelian topological order, including quantum doubles for solvable groups. A natural question is to find an analogue for non-solvable groups—or to prove a no-go theorem. We also argued that non-Abelian states beyond quantum doubles can be obtained, such as the doubled Ising anyon theory, although we have left an explicit prescription of a circuit to future work.

Another feature of our method is that it can be performed in an arbitrary region, producing a duality defect on its boundary. We expect this defect to be topological [127–129]. Perhaps it is natural to consider moving it by measurements?

It is also interesting to note the similarities to quantum teleportation [130] and measurement-based quantum computation (MBQC) [131–134], where measurement effectively performs unitary operations on the input state. Here, the act of measurement instead performs a non-local transformation on the initial state. It would be interesting to make contact with similar notions of "computational phases of matter" in MBQC [135–139] . Exploring connections to the topological bootstrap [140] is also a promising future direction.

It may also be interesting to "soften" the projectors, considering either weak measurements or an open system weakly interacting with the environment by a subset of its degrees of freedom.

Note added: On completion of the present work, Ref. [141] appeared, which overlaps with our section on

KW duality. Our results agree where they intersect.

Note added in second version: After our preprint appeared, we learnt of parallel work preparing quantum double topological order via measurements [142]. Our results agree where they intersect.

ACKNOWLEDGMENTS

We thank David T. Stephen for insightful observations about measurement-based preparation of non-Abelian topological order. DMRG simulations were performed using the TeNPy Library [124]. NT is supported by NSERC. RV and AV are supported by the Simons Collaboration on Ultra-Quantum Matter, which is a grant from the Simons Foundation (651440, A.V.). RV is supported by the Harvard Quantum Initiative Postdoctoral Fellowship in Science and Engineering.

[1] S. Bravyi, M. B. Hastings, and F. Verstraete, Lieb-robinson bounds and the generation of correlations and topological quantum order, Phys. Rev. Lett. **97**, 050401 (2006).
[2] M. B. Hastings, Locality in quantum systems, in *Quantum Theory from Small to Large Scales*, Les Houches 2010, Session 95 (Oxford University Press, 2012) pp. 171–212.
[3] X. Chen, Z.-C. Gu, and X.-G. Wen, Classification of gapped symmetric phases in one-dimensional spin systems, Phys. Rev. B **83**, 035107 (2011).
[4] X. Chen, Z.-C. Gu, and X.-G. Wen, Complete classification of one-dimensional gapped quantum phases in interacting spin systems, Phys. Rev. B **84**, 235128 (2011).
[5] B. Zeng and X.-G. Wen, Gapped quantum liquids and topological order, stochastic local transformations and emergence of unitarity, Phys. Rev. B **91**, 125121 (2015).
[6] Y. Huang and X. Chen, Quantum circuit complexity of one-dimensional topological phases, Phys. Rev. B **91**, 195143 (2015).
[7] J. Haah, An invariant of topologically ordered states under local unitary transformations, Communications in Mathematical Physics **342**, 771 (2016).
[8] N. Read and S. Sachdev, Large-n expansion for frustrated quantum antiferromagnets, Phys. Rev. Lett. **66**, 1773 (1991).
[9] X.-G. Wen, Topological orders in rigid states, International Journal of Modern Physics B **4**, 239 (1990).
[10] X. Wen, *Quantum Field Theory of Many-body Systems*, Oxford graduate texts (Oxford University Press, 2004).
[11] J. Fuchs, I. Runkel, and C. Schweigert, Tft construction of rcft correlators i: partition functions, Nuclear Physics B **646**, 353?497 (2002).
[12] A. Kitaev, Fault-tolerant quantum computation by anyons, Annals of Physics **303**, 2?30 (2003).
[13] A. Kitaev, Anyons in an exactly solved model and beyond, Annals of Physics **321**, 2 (2006).
[14] C. Chamon, Quantum glassiness in strongly correlated clean systems: An example of topological overprotection, Phys. Rev. Lett. **94**, 040402 (2005).
[15] J. Haah, Local stabilizer codes in three dimensions without string logical operators, Phys. Rev. A **83**, 042330 (2011).
[16] B. Yoshida, Exotic topological order in fractal spin liquids, Phys. Rev. B **88**, 125122 (2013).
[17] S. Vijay, J. Haah, and L. Fu, A new kind of topological quantum order: A dimensional hierarchy of quasiparticles built from stationary excitations, Phys. Rev. B **92**, 235136 (2015).
[18] S. Vijay, J. Haah, and L. Fu, Fracton topological order, generalized lattice gauge theory, and duality, Phys. Rev. B **94**, 235157 (2016).
[19] R. M. Nandkishore and M. Hermele, Fractons, Annual Review of Condensed Matter Physics **10**, 295 (2019).
[20] M. Pretko, X. Chen, and Y. You, Fracton phases of matter, International Journal of Modern Physics A **35**, 2030003 (2020).
[21] Z.-C. Gu and X.-G. Wen, Tensor-entanglement-filtering renormalization approach and symmetry-protected topological order, Phys. Rev. B **80**, 155131 (2009).
[22] F. Pollmann, A. M. Turner, E. Berg, and M. Oshikawa, Entanglement spectrum of a topological phase in one dimension, Phys. Rev. B **81**, 064439 (2010).
[23] L. Fidkowski and A. Kitaev, Topological phases of fermions in one dimension, Physical Review B **83**, 10.1103/physrevb.83.075103 (2011).
[24] A. M. Turner, F. Pollmann, and E. Berg, Topological phases of one-dimensional fermions: An entanglement point of view, Phys. Rev. B **83**, 075102 (2011).
[25] N. Schuch, D. Pérez-García, and I. Cirac, Classifying quantum phases using matrix product states and projected entangled pair states, Phys. Rev. B **84**, 165139 (2011).
[26] X. Chen, Z.-X. Liu, and X.-G. Wen, Two-dimensional symmetry-protected topological orders and their protected gapless edge excitations, Phys. Rev. B **84**, 235141 (2011).
[27] X. Chen, Z.-C. Gu, Z.-X. Liu, and X.-G. Wen, Symmetry protected topological orders and the group cohomology of their symmetry group, Physical Review B **87**, 10.1103/physrevb.87.155114 (2013).
[28] F. Pollmann, E. Berg, A. M. Turner, and M. Oshikawa, Symmetry protection of topological phases in one-dimensional quantum spin systems, Phys. Rev. B **85**, 075125 (2012).
[29] Y.-M. Lu and A. Vishwanath, Theory and classification of interacting integer topological phases in two dimensions: A chern-simons approach, Phys. Rev. B **86**, 125119 (2012).
[30] T. Senthil and M. Levin, Integer quantum hall effect for bosons, Phys. Rev. Lett. **110**, 046801 (2013).
[31] M. Levin and Z.-C. Gu, Braiding statistics approach to symmetry-protected topological phases, Phys. Rev. B **86**, 115109 (2012).

[32] A. Vishwanath and T. Senthil, Physics of three-dimensional bosonic topological insulators: Surface-deconfined criticality and quantized magnetoelectric effect, Phys. Rev. X **3**, 011016 (2013).

[33] D. V. Else and C. Nayak, Classifying symmetry-protected topological phases through the anomalous action of the symmetry on the edge, Phys. Rev. B **90**, 235137 (2014).

[34] Y. Li, X. Chen, and M. P. A. Fisher, Quantum zeno effect and the many-body entanglement transition, Phys. Rev. B **98**, 205136 (2018).

[35] B. Skinner, J. Ruhman, and A. Nahum, Measurement-induced phase transitions in the dynamics of entanglement, Phys. Rev. X **9**, 031009 (2019).

[36] A. Chan, R. M. Nandkishore, M. Pretko, and G. Smith, Unitary-projective entanglement dynamics, Phys. Rev. B **99**, 224307 (2019).

[37] Y. Li, X. Chen, and M. P. A. Fisher, Measurement-driven entanglement transition in hybrid quantum circuits, Phys. Rev. B **100**, 134306 (2019).

[38] R. Vasseur, A. C. Potter, Y.-Z. You, and A. W. W. Ludwig, Entanglement transitions from holographic random tensor networks, Phys. Rev. B **100**, 134203 (2019).

[39] X. Cao, A. Tilloy, and A. D. Luca, Entanglement in a fermion chain under continuous monitoring, SciPost Phys. **7**, 24 (2019).

[40] M. J. Gullans and D. A. Huse, Dynamical purification phase transition induced by quantum measurements, Phys. Rev. X **10**, 041020 (2020).

[41] S. Choi, Y. Bao, X.-L. Qi, and E. Altman, Quantum error correction in scrambling dynamics and measurement-induced phase transition, Phys. Rev. Lett. **125**, 030505 (2020).

[42] Q. Tang and W. Zhu, Measurement-induced phase transition: A case study in the nonintegrable model by density-matrix renormalization group calculations, Phys. Rev. Research **2**, 013022 (2020).

[43] C.-M. Jian, Y.-Z. You, R. Vasseur, and A. W. W. Ludwig, Measurement-induced criticality in random quantum circuits, Phys. Rev. B **101**, 104302 (2020).

[44] J. Lopez-Piqueres, B. Ware, and R. Vasseur, Mean-field entanglement transitions in random tree tensor networks, Phys. Rev. B **102**, 064202 (2020).

[45] Y. Bao, S. Choi, and E. Altman, Theory of the phase transition in random unitary circuits with measurements, Phys. Rev. B **101**, 104301 (2020).

[46] D. Rossini and E. Vicari, Measurement-induced dynamics of many-body systems at quantum criticality, Phys. Rev. B **102**, 035119 (2020).

[47] L. Piroli, C. Sünderhauf, and X.-L. Qi, A random unitary circuit model for black hole evaporation, Journal of High Energy Physics **2020**, 1 (2020).

[48] R. Fan, S. Vijay, A. Vishwanath, and Y.-Z. You, Self-organized error correction in random unitary circuits with measurement, Phys. Rev. B **103**, 174309 (2021).

[49] Y. Li, X. Chen, A. W. W. Ludwig, and M. P. A. Fisher, Conformal invariance and quantum nonlocality in critical hybrid circuits, Phys. Rev. B **104**, 104305 (2021).

[50] D. Ben-Zion, J. McGreevy, and T. Grover, Disentangling quantum matter with measurements, Phys. Rev. B **101**, 115131 (2020).

[51] H. J. Briegel and R. Raussendorf, Persistent entanglement in arrays of interacting particles, Phys. Rev. Lett. **86**, 910 (2001).

[52] R. Raussendorf, S. Bravyi, and J. Harrington, Long-range quantum entanglement in noisy cluster states, Phys. Rev. A **71**, 062313 (2005).

[53] M. Aguado, G. K. Brennen, F. Verstraete, and J. I. Cirac, Creation, manipulation, and detection of abelian and non-abelian anyons in optical lattices, Phys. Rev. Lett. **101**, 260501 (2008).

[54] L. Piroli, G. Styliaris, and J. I. Cirac, Quantum circuits assisted by local operations and classical communication: Transformations and phases of matter, Phys. Rev. Lett. **127**, 220503 (2021).

[55] A. T. Schmitz, Distilling fractons from layered subsystem-symmetry protected phases, arXiv preprint arXiv:1910.04765 (2019).

[56] D. J. Williamson and T. Devakul, Type-ii fractons from coupled spin chains and layers, Phys. Rev. B **103**, 155140 (2021).

[57] A. R. Calderbank and P. W. Shor, Good quantum error-correcting codes exist, Phys. Rev. A **54**, 1098 (1996).

[58] A. Steane, Multiple-particle interference and quantum error correction, Proceedings of the Royal Society of London. Series A: Mathematical, Physical and Engineering Sciences **452**, 2551 (1996).

[59] A. Bolt, G. Duclos-Cianci, D. Poulin, and T. M. Stace, Foliated quantum error-correcting codes, Phys. Rev. Lett. **117**, 070501 (2016).

[60] Y. Hu, Y. Wan, and Y.-S. Wu, Twisted quantum double model of topological phases in two dimensions, Phys. Rev. B **87**, 125114 (2013).

[61] H. Song, A. Prem, S.-J. Huang, and M. A. Martin-Delgado, Twisted fracton models in three dimensions, Phys. Rev. B **99**, 155118 (2019).

[62] D. Bulmash and M. Barkeshli, Gauging fractons: Immobile non-abelian quasiparticles, fractals, and position-dependent degeneracies, Phys. Rev. B **100**, 155146 (2019).

[63] A. Prem and D. J. Williamson, Gauging permutation symmetries as a route to non-Abelian fractons, SciPost Phys. **7**, 68 (2019).

[64] D. Aasen, D. Bulmash, A. Prem, K. Slagle, and D. J. Williamson, Topological defect networks for fractons of all types, Phys. Rev. Research **2**, 043165 (2020).

[65] D. T. Stephen, J. Garre-Rubio, A. Dua, and D. J. Williamson, Subsystem symmetry enriched topological order in three dimensions, Phys. Rev. Research **2**, 033331 (2020).

[66] X.-G. Wen, Systematic construction of gapped nonliquid states, Phys. Rev. Research **2**, 033300 (2020).

[67] J. Wang, Non-liquid cellular states, arXiv preprint arXiv:2002.12932 (2020).

[68] D. J. Williamson and M. Cheng, Designer non-abelian fractons from topological layers, arXiv preprint arXiv:2004.07251 (2020).

[69] N. Tantivasadakarn, W. Ji, and S. Vijay, Non-abelian hybrid fracton orders, Phys. Rev. B **104**, 115117 (2021).

[70] F. J. Wegner, Duality in generalized ising models and phase transitions without local order parameters, J. Math. Phys. **12**, 2259 (1971).

[71] J. B. Kogut, An introduction to lattice gauge theory and spin systems, Rev. Mod. Phys. **51**, 659 (1979).

[72] E. Cobanera, G. Ortiz, and Z. Nussinov, The bond-algebraic approach to dualities, Advances in physics **60**, 679 (2011).

[73] D. J. Williamson, Fractal symmetries: Ungauging the

cubic code, Phys. Rev. B **94**, 155128 (2016).
[74] A. Kubica and B. Yoshida, Ungauging quantum error-correcting codes, arXiv preprint arXiv:1805.01836 (2018).
[75] M. Pretko, The fracton gauge principle, Phys. Rev. B **98**, 115134 (2018).
[76] W. Shirley, K. Slagle, and X. Chen, Foliated fracton order from gauging subsystem symmetries, SciPost Phys. **6**, 41 (2019).
[77] D. Radicevic, Systematic constructions of fracton theories, arXiv preprint arXiv:1910.06336 (2019).
[78] P. Jordan and E. Wigner, Uber das paulische equivalenzverbot, Zeitschrift fur Physik **47**, 631 (1928).
[79] T. D. Schultz, D. C. Mattis, and E. H. Lieb, Two-dimensional ising model as a soluble problem of many fermions, Rev. Mod. Phys. **36**, 856 (1964).
[80] Y.-A. Chen, A. Kapustin, and D. Radicevic, Exact bosonization in two spatial dimensions and a new class of lattice gauge theories, Annals of Physics **393**, 234 (2018).
[81] Y.-A. Chen and A. Kapustin, Bosonization in three spatial dimensions and a 2-form gauge theory, Phys. Rev. B **100**, 245127 (2019).
[82] Y.-A. Chen, Exact bosonization in arbitrary dimensions, Phys. Rev. Research **2**, 033527 (2020).
[83] N. Tantivasadakarn, Jordan-wigner dualities for translation-invariant hamiltonians in any dimension: Emergent fermions in fracton topological order, Phys. Rev. Research **2**, 023353 (2020).
[84] W. Shirley, Fractonic order and emergent fermionic gauge theory, arXiv preprint arXiv:2002.12026 (2020).
[85] H. C. Po, Symmetric jordan-wigner transformation in higher dimensions, arXiv preprint arXiv:2107.10842 (2021).
[86] K. Li and H. C. Po, Higher-dimensional jordan-wigner transformation and auxiliary majorana fermions, arXiv preprint arXiv:2107.14083 (2021).
[87] R. Verresen, N. Tantivasadakarn, and A. Vishwanath, Efficiently preparing schrödinger's cat, fractons and non-abelian topological order in quantum devices, arXiv preprint arXiv:2112.03061 (2021).
[88] R. A. Fisher, Theory of statistical estimation, Mathematical Proceedings of the Cambridge Philosophical Society **22**, 700?725 (1925).
[89] V. Giovannetti, S. Lloyd, and L. Maccone, Quantum metrology, Phys. Rev. Lett. **96**, 010401 (2006).
[90] F. Verstraete, M. M. Wolf, D. Perez-Garcia, and J. I. Cirac, Criticality, the area law, and the computational power of projected entangled pair states, Phys. Rev. Lett. **96**, 220601 (2006).
[91] J. I. Cirac, D. Pérez-García, N. Schuch, and F. Verstraete, Matrix product states and projected entangled pair states: Concepts, symmetries, theorems, Rev. Mod. Phys. **93**, 045003 (2021).
[92] D. J. Williamson, C. Delcamp, F. Verstraete, and N. Schuch, On the stability of topological order in tensor network states, Phys. Rev. B **104**, 235151 (2021).
[93] C. Delcamp and N. Schuch, On tensor network representations of the (3+ 1) d toric code, Quantum **5**, 604 (2021).
[94] C. Vafa, Modular invariance and discrete torsion on orbifolds, Nuclear Physics B **273**, 592 (1986).
[95] M. Barkeshli, P. Bonderson, M. Cheng, and Z. Wang, Symmetry fractionalization, defects, and gauging of topological phases, Phys. Rev. B **100**, 115147 (2019).
[96] M. de Wild Propitius, *Topological interactions in broken gauge theories*, Ph.D. thesis, - (1995).
[97] B. Yoshida, Topological phases with generalized global symmetries, Phys. Rev. B **93**, 155131 (2016).
[98] W. Shirley, K. Slagle, and X. Chen, Twisted foliated fracton phases, Phys. Rev. B **102**, 115103 (2020).
[99] T. Devakul, W. Shirley, and J. Wang, Strong planar subsystem symmetry-protected topological phases and their dual fracton orders, Phys. Rev. Research **2**, 012059 (2020).
[100] P. Ginsparg, Applied conformal field theory, in *Fields, Strings and Critical Phenomena*, Les Houches 1988, Session 49, edited by J. Zinn-Justin and E. Brézin (North-Holland, 1989).
[101] G. Brennen, M. Aguado, and J. I. Cirac, Simulations of quantum double models, New Journal of Physics **11**, 053009 (2009).
[102] C. G. Brell, Generalized cluster states based on finite groups, New Journal of Physics **17**, 023029 (2015).
[103] J. Haegeman, K. Van Acoleyen, N. Schuch, J. I. Cirac, and F. Verstraete, Gauging quantum states: From global to local symmetries in many-body systems, Phys. Rev. X **5**, 011024 (2015).
[104] C. Mochon, Anyon computers with smaller groups, Phys. Rev. A **69**, 032306 (2004).
[105] C. Heinrich, F. Burnell, L. Fidkowski, and M. Levin, Symmetry-enriched string nets: Exactly solvable models for set phases, Phys. Rev. B **94**, 235136 (2016).
[106] M. Cheng, Z.-C. Gu, S. Jiang, and Y. Qi, Exactly solvable models for symmetry-enriched topological phases, Phys. Rev. B **96**, 115107 (2017).
[107] Z.-C. Gu and X.-G. Wen, Symmetry-protected topological orders for interacting fermions: Fermionic topological nonlinear σ models and a special group supercohomology theory, Phys. Rev. B **90**, 115141 (2014).
[108] C. W. von Keyserlingk and S. L. Sondhi, Phase structure of one-dimensional interacting floquet systems. i. abelian symmetry-protected topological phases, Phys. Rev. B **93**, 245145 (2016).
[109] N. Tantivasadakarn and A. Vishwanath, Full commuting projector hamiltonians of interacting symmetry-protected topological phases of fermions, Phys. Rev. B **98**, 165104 (2018).
[110] U. Borla, R. Verresen, J. Shah, and S. Moroz, Gauging the Kitaev chain, SciPost Phys. **10**, 148 (2021).
[111] D. Gaiotto and A. Kapustin, Spin tqfts and fermionic phases of matter, International Journal of Modern Physics A **31**, 1645044 (2016).
[112] S. K. Shukla, T. D. Ellison, and L. Fidkowski, Tensor network approach to two-dimensional bosonization, Phys. Rev. B **101**, 155105 (2020).
[113] P. Smacchia, L. Amico, P. Facchi, R. Fazio, G. Florio, S. Pascazio, and V. Vedral, Statistical mechanics of the cluster ising model, Phys. Rev. A **84**, 022304 (2011).
[114] F. Pollmann and A. M. Turner, Detection of symmetry-protected topological phases in one dimension, Phys. Rev. B **86**, 125441 (2012).
[115] I. Marvian, Symmetry-protected topological entanglement, Phys. Rev. B **95**, 045111 (2017).
[116] D. Gaiotto, A. Kapustin, N. Seiberg, and B. Willett, Generalized global symmetries, Journal of High Energy Physics **2015**, 10.1007/jhep02(2015)172 (2015).
[117] A. Kapustin and R. Thorngren, Higher symmetry and

gapped phases of gauge theories, in *Algebra, Geometry, and Physics in the 21st Century* (Springer, 2017) pp. 177–202.

[118] F. Haldane, Continuum dynamics of the 1-d heisenberg antiferromagnet: Identification with the o(3) nonlinear sigma model, Physics Letters A **93**, 464 (1983).

[119] I. Affleck, T. Kennedy, E. H. Lieb, and H. Tasaki, Rigorous results on valence-bond ground states in antiferromagnets, Phys. Rev. Lett. **59**, 799 (1987).

[120] M. den Nijs and K. Rommelse, Preroughening transitions in crystal surfaces and valence-bond phases in quantum spin chains, Phys. Rev. B **40**, 4709 (1989).

[121] F. Pollmann, A. M. Turner, E. Berg, and M. Oshikawa, Entanglement spectrum of a topological phase in one dimension, Phys. Rev. B **81**, 064439 (2010).

[122] S. R. White, Density matrix formulation for quantum renormalization groups, Phys. Rev. Lett. **69**, 2863 (1992).

[123] S. R. White, Density-matrix algorithms for quantum renormalization groups, Phys. Rev. B **48**, 10345 (1993).

[124] J. Hauschild and F. Pollmann, Efficient numerical simulations with Tensor Networks: Tensor Network Python (TeNPy), SciPost Phys. Lect. Notes , 5 (2018).

[125] B. Yoshida, Topological color code and symmetry-protected topological phases, Phys. Rev. B **91**, 245131 (2015).

[126] X. Chen, Y.-M. Lu, and A. Vishwanath, Symmetry-protected topological phases from decorated domain walls, Nature communications **5**, 3507 (2014).

[127] J. Fröhlich, J. Fuchs, I. Runkel, and C. Schweigert, Kramers-wannier duality from conformal defects, Phys. Rev. Lett. **93**, 070601 (2004).

[128] D. Aasen, R. S. K. Mong, and P. Fendley, Topological defects on the lattice: I. the ising model, Journal of Physics A: Mathematical and Theoretical **49**, 354001 (2016).

[129] C.-M. Chang, Y.-H. Lin, S.-H. Shao, Y. Wang, and X. Yin, Topological defect lines and renormalization group flows in two dimensions, Journal of High Energy Physics **2019**, 1 (2019).

[130] C. H. Bennett, G. Brassard, C. Crépeau, R. Jozsa, A. Peres, and W. K. Wootters, Teleporting an unknown quantum state via dual classical and einstein-podolsky-rosen channels, Phys. Rev. Lett. **70**, 1895 (1993).

[131] D. Gottesman and I. L. Chuang, Demonstrating the viability of universal quantum computation using teleportation and single-qubit operations, Nature **402**, 390 (1999).

[132] H. J. Briegel and R. Raussendorf, Persistent entanglement in arrays of interacting particles, Phys. Rev. Lett. **86**, 910 (2001).

[133] R. Raussendorf and H. J. Briegel, A one-way quantum computer, Phys. Rev. Lett. **86**, 5188 (2001).

[134] R. Raussendorf, D. E. Browne, and H. J. Briegel, Measurement-based quantum computation on cluster states, Phys. Rev. A **68**, 022312 (2003).

[135] R. Raussendorf, D.-S. Wang, A. Prakash, T.-C. Wei, and D. T. Stephen, Symmetry-protected topological phases with uniform computational power in one dimension, Phys. Rev. A **96**, 012302 (2017).

[136] R. Raussendorf, C. Okay, D.-S. Wang, D. T. Stephen, and H. P. Nautrup, Computationally universal phase of quantum matter, Phys. Rev. Lett. **122**, 090501 (2019).

[137] D. T. Stephen, D.-S. Wang, A. Prakash, T.-C. Wei, and R. Raussendorf, Computational power of symmetry-protected topological phases, Phys. Rev. Lett. **119**, 010504 (2017).

[138] T. Devakul and D. J. Williamson, Universal quantum computation using fractal symmetry-protected cluster phases, Phys. Rev. A **98**, 022332 (2018).

[139] A. K. Daniel, R. N. Alexander, and A. Miyake, Computational universality of symmetry-protected topologically ordered cluster phases on 2D Archimedean lattices, Quantum **4**, 228 (2020).

[140] T. H. Hsieh, Y.-M. Lu, and A. W. Ludwig, Topological bootstrap: Fractionalization from kondo coupling, Science advances **3**, e1700729 (2017).

[141] S. Ashkenazi and E. Zohar, Duality as a feasible physical transformation (2021), arXiv:2111.04765 [quant-ph].

[142] S. Bravyi, I. Kim, A. Kliesch, and R. Koenig, To appear.

[143] T. Devakul, D. J. Williamson, and Y. You, Classification of subsystem symmetry-protected topological phases, Phys. Rev. B **98**, 235121 (2018).

[144] N. Tantivasadakarn and S. Vijay, Searching for fracton orders via symmetry defect condensation, Phys. Rev. B **101**, 165143 (2020).

[145] A. Kitaev and L. Kong, Models for gapped boundaries and domain walls, Communications in Mathematical Physics **313**, 351 (2012).

[146] F. J. Burnell, X. Chen, L. Fidkowski, and A. Vishwanath, Exactly soluble model of a three-dimensional symmetry-protected topological phase of bosons with surface topological order, Phys. Rev. B **90**, 245122 (2014).

[147] J. Haah, L. Fidkowski, and M. B. Hastings, Nontrivial Quantum Cellular Automata in Higher Dimensions, arXiv:1812.01625 (2018).

[148] K. Walker and Z. Wang, (3+1)-tqfts and topological insulators, Frontiers of Physics **7**, 150 (2012).

[149] R. Raussendorf, J. Harrington, and K. Goyal, A fault-tolerant one-way quantum computer, Annals of Physics **321**, 2242 (2006).

[150] S. Roberts and D. J. Williamson, 3-fermion topological quantum computation, arXiv preprint arXiv:2011.04693 (2020).

[151] Y.-A. Chen and S. Tata, Higher cup products on hypercubic lattices: application to lattice models of topological phases, arXiv preprint arXiv:2106.05274 (2021).

[152] J. Haah, Commuting pauli hamiltonians as maps between free modules, Communications in Mathematical Physics **324**, 351?399 (2013).

[153] L. Tsui and X.-G. Wen, Lattice models that realize $\mathbb{Z}_n$-1 symmetry-protected topological states for even n, Phys. Rev. B **101**, 035101 (2020).

[154] R. Raussendorf, S. Bravyi, and J. Harrington, Long-range quantum entanglement in noisy cluster states, Phys. Rev. A **71**, 062313 (2005).

[155] Q.-R. Wang, Y. Qi, and Z.-C. Gu, Anomalous symmetry protected topological states in interacting fermion systems, Phys. Rev. Lett. **123**, 207003 (2019).

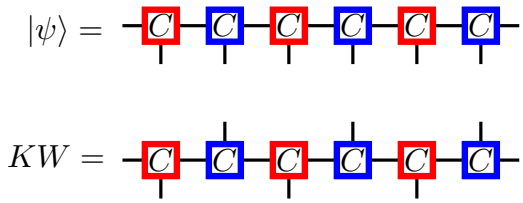

FIG. 6. The KW MPO is obtained by starting with the MPS of the 1D cluster state flipping the legs on the B (blue) sublattice. Generalized KW dualities can be similarly obtained by a cluster state which is a non-trivial SPT protected by the desired symmetries on a bipartite lattice.

Appendix A: Matrix product for the 1D cluster state and KW

Consider a one-dimensional lattice of $2N$ qubits. We identify two sublattices A and B corresponding to the odd and even sites of the lattice, respectively. The 1D cluster state can be expressed using a Matrix Product State (MPS) as

$$|\psi\rangle = \sum_{\{s\}} \mathrm{Tr}[C^{s_1} C^{s_2} \cdots C^{s_{2N}}] \, |s_1, s_2, ..., s_{2N}\rangle \tag{A1}$$

where $s_n = 0, 1$ are Z-basis states and the tensor C is defined as

$$C = \frac{1}{\sqrt{2}} \begin{pmatrix} \langle 0| & \langle 0| \\ \langle 1| & \langle -1| \end{pmatrix} \tag{A2}$$

To turn this into a Matrix Product Operator (MPO), we first double the unit cell to get an MPS with double the physical legs.

$$C \otimes C = \begin{pmatrix} \langle 0+| & \langle 1-| \\ \langle 0-| & \langle 1+| \end{pmatrix} \tag{A3}$$

Flipping the leg of the first entry upwards yields the MPO

$$\sigma = \begin{pmatrix} |0\rangle\langle +| & |1\rangle\langle -| \\ |0\rangle\langle -| & |1\rangle\langle +| \end{pmatrix} \tag{A4}$$

This is exactly the Kramers-Wannier duality. For example, if we plug in the $|+\rangle$ product state, then we get the MPS for the GHZ state

$$\begin{pmatrix} \langle 0| & 0 \\ 0 & \langle 1| \end{pmatrix} \tag{A5}$$

Appendix B: More examples

1. Wen plaquette model

Consider the following cluster state given by stabilizers

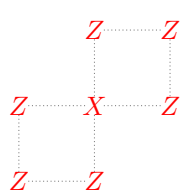

(B1)

This is in fact the cluster state on the triangular lattice, although we have placed it on the square lattice. This cluster state is a (strong) $\mathbb{Z}_2$ subsystem SPT protected by line symmetries, given by flipping spins along the x and y lines of the square lattice [143]. In fact, gauging this subsystem SPT gives rise to the Wen plaquette model[144].

Based on this, we show how to prepare the Wen plaquette model via measuring an appropriate cluster state. The A and B are the vertices of the square (red) and dual square (blue) sublattices, respectively. We create the cluster state given by stabilizers

(B2)

Note that because of the couplings within the A sublattice, this cluster state is not bipartite. Now, let us measure the X operators on the A sublattice. The local product of stabilizers that commute with the measurements are

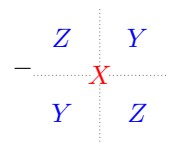

(B3)

and the non-local products are $\prod X$ along each x and y lines.

Thus with measurement outcomes $X = (-1)^{s-v}$ we have the stabilizers

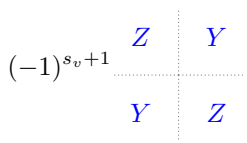

(B4)

which up to single site rotations, are the stabilizers of the Wen plaquette model.

Although the Wen plaquette model is in the same topological phase as the toric code, it has the advantage of treating the e and m anyons on equal footing. In particular, it naturally has a dislocation defect which permutes the e and m anyons that encircles the defect [145]. In other words, the dislocation hosts a Majorana zero mode. Consider the cluster state given by the graph

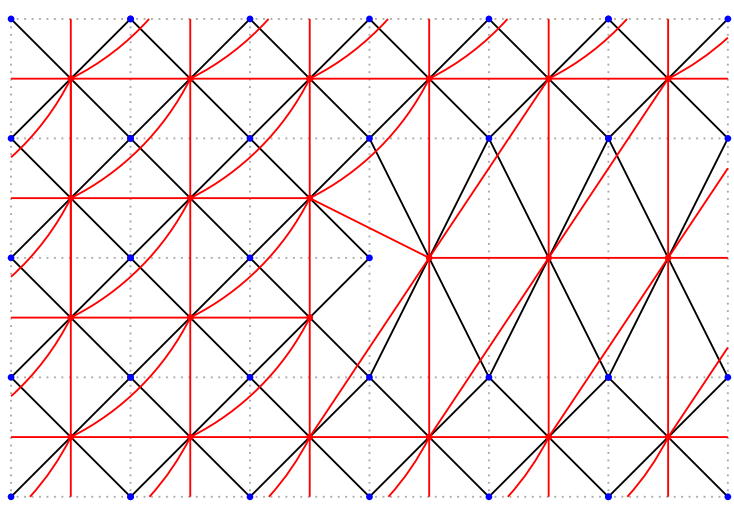

which features a dislocation on the B sublattice (dotted lines). Here the black lines connect AB sites, while the red lines connect AA sites. Performing measurements on the A sublattice, the stabilizers for each plaquettes on the blue sites is given by

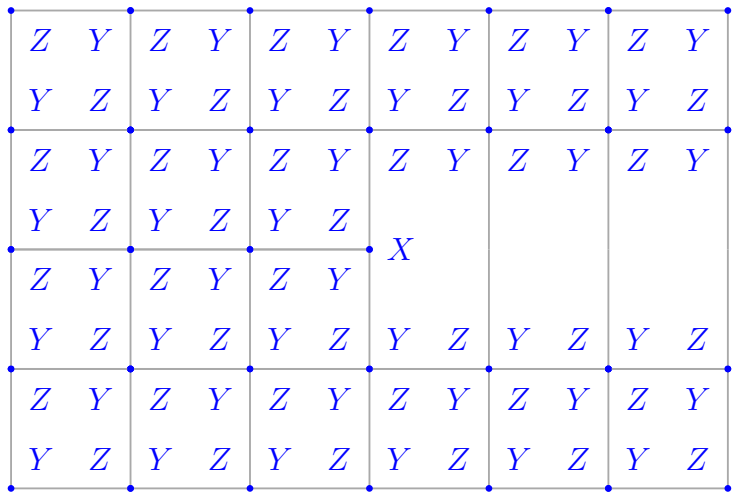

2. 3-Fermion Walker-Wang model

It is argued that the 3-Fermion Walker-Wang (3FWW) model[146] cannot be created from a circuit; it requires a Quantum Cellular Automaton[147]. Here, we argue that we can alternatively create this state by measuring an appropriate 3D cluster state. The preparation of such state can prove useful for measurement based quantum computation using such Walker-Wang models[148] by effectively evolving the two dimensional topological order on the boundary using measurements[149, 150].

The 3FWW model can be obtained by gauging a $\mathbb{Z}_2^2$ 1-form SPT[151]. The response of this SPT to background $\mathbb{Z}_2$ 2-form gauge fields B_1 and B_2 is given by $B_1^2 + B_2^2 + B_1 B_2$. The physical interpretation of the three terms is that it statistically transmutes the anyons on the boundary to become that of fermions.

Conveniently, the above SPT phase is itself a cluster state. Therefore combining with the cluster state that implements the KW duality on each sublattice, the cluster state we perform the measurement to obtain the 3FWW is a $\mathbb{Z}_2^4$ 1-form SPT. Its response to background gauge fields B_i for $i = 1, 2, 3, 4$ is $B_1^2 + B_2^2 + B_1 B_2 + B_1 B_4 + B_2 B_3$. The 3FWW is obtained by measuring the 1 and 2 sublattices.

Because it is a 1-form SPT, we define the cluster state on the edges of a cubic lattice, with four qubits placed per edge (i.e. twelve sites per unit cell). It is convenient to describe the cluster state using polynomials[152], which denote the connectivity of this cluster state.

As a stepping stone, we describe the stabilizers for the B^2 SPT

$$\left(\begin{array}{ccc} 0 & (y+\bar{z}\bar{x})(1+z) & (z+\bar{x}\bar{y})(1+y) \\ (x+\bar{y}\bar{z})(1+z) & 0 & (z+\bar{x}\bar{y})(1+x) \\ (x+\bar{y}\bar{z})(1+y) & (y+\bar{z}\bar{x})(1+x) & 0 \\ \hline 1 & 0 & 0 \\ 0 & 1 & 0 \\ 0 & 0 & 1 \end{array}\right) \tag{B5}$$

Here, each column denotes a stabilizer, and the top/bottom rows denotes the positions of the Pauli-Z and Pauli-X's,

respectively. Similarly the B_1B_2 SPT (RBH cluster state) [97, 153, 154] has stabilizers

$$\left(\begin{array}{cccccc}
0 & 0 & 0 & 0 & \bar{x}(1+\bar{z}) & \bar{x}(1+\bar{y}) \\
0 & 0 & 0 & \bar{y}(1+z) & 0 & \bar{y}(1+\bar{x}) \\
0 & 0 & 0 & \bar{z}(1+\bar{y}) & \bar{x}(1+\bar{y}) & 0 \\
0 & y(1+z) & z(1+y) & 0 & 0 & 0 \\
x(1+z) & 0 & z(1+x) & 0 & 0 & 0 \\
x(1+y) & y(1+x) & 0 & 0 & 0 & 0 \\
\hline
1 & 0 & 0 & 0 & 0 & 0 \\
0 & 1 & 0 & 0 & 0 & 0 \\
0 & 0 & 1 & 0 & 0 & 0 \\
0 & 0 & 0 & 1 & 0 & 0 \\
0 & 0 & 0 & 0 & 1 & 0 \\
0 & 0 & 0 & 0 & 0 & 1
\end{array}\right) \tag{B6}$$

Therefore our desired cluster state is given by the stabilizers

$$\left(\begin{array}{cccccccccccc}
0 & (y+\bar{z}\bar{x})(1+z) & (z+\bar{x}\bar{y})(1+y) & 0 & \bar{x}(1+\bar{z}) & \bar{x}(1+\bar{y}) & 0 & 0 & 0 & 0 & \bar{x}(1+\bar{z}) & \bar{x}(1+\bar{y}) \\
(x+\bar{y}\bar{z})(1+z) & 0 & (z+\bar{x}\bar{y})(1+x) & \bar{y}(1+z) & 0 & \bar{y}(1+\bar{x}) & 0 & 0 & 0 & \bar{y}(1+z) & 0 & \bar{y}(1+\bar{x}) \\
(x+\bar{y}\bar{z})(1+y) & (y+\bar{z}\bar{x})(1+x) & 0 & \bar{z}(1+\bar{y}) & \bar{x}(1+\bar{y}) & 0 & 0 & 0 & 0 & \bar{z}(1+\bar{y}) & \bar{x}(1+\bar{y}) & 0 \\
0 & y(1+z) & z(1+y) & 0 & (y+\bar{z}\bar{x})(1+z) & (z+\bar{x}\bar{y})(1+y) & 0 & \bar{x}(1+\bar{z}) & \bar{x}(1+\bar{y}) & 0 & 0 & 0 \\
x(1+z) & 0 & z(1+x) & (x+\bar{y}\bar{z})(1+z) & 0 & (z+\bar{x}\bar{y})(1+x) & \bar{y}(1+z) & 0 & \bar{y}(1+\bar{x}) & 0 & 0 & 0 \\
x(1+y) & y(1+x) & 0 & (x+\bar{y}\bar{z})(1+y) & (y+\bar{z}\bar{x})(1+x) & 0 & \bar{z}(1+\bar{y}) & \bar{x}(1+\bar{y}) & 0 & 0 & 0 & 0 \\
0 & 0 & 0 & 0 & y(1+z) & z(1+y) & 0 & 0 & 0 & 0 & 0 & 0 \\
0 & 0 & 0 & x(1+z) & 0 & z(1+x) & 0 & 0 & 0 & 0 & 0 & 0 \\
0 & 0 & 0 & x(1+y) & y(1+x) & 0 & 0 & 0 & 0 & 0 & 0 & 0 \\
0 & y(1+z) & z(1+y) & 0 & 0 & 0 & 0 & 0 & 0 & 0 & 0 & 0 \\
x(1+z) & 0 & z(1+x) & 0 & 0 & 0 & 0 & 0 & 0 & 0 & 0 & 0 \\
x(1+y) & y(1+x) & 0 & 0 & 0 & 0 & 0 & 0 & 0 & 0 & 0 & 0 \\
\hline
1 & 0 & 0 & 0 & 0 & 0 & 0 & 0 & 0 & 0 & 0 & 0 \\
0 & 1 & 0 & 0 & 0 & 0 & 0 & 0 & 0 & 0 & 0 & 0 \\
0 & 0 & 1 & 0 & 0 & 0 & 0 & 0 & 0 & 0 & 0 & 0 \\
0 & 0 & 0 & 1 & 0 & 0 & 0 & 0 & 0 & 0 & 0 & 0 \\
0 & 0 & 0 & 0 & 1 & 0 & 0 & 0 & 0 & 0 & 0 & 0 \\
0 & 0 & 0 & 0 & 0 & 1 & 0 & 0 & 0 & 0 & 0 & 0 \\
0 & 0 & 0 & 0 & 0 & 0 & 1 & 0 & 0 & 0 & 0 & 0 \\
0 & 0 & 0 & 0 & 0 & 0 & 0 & 1 & 0 & 0 & 0 & 0 \\
0 & 0 & 0 & 0 & 0 & 0 & 0 & 0 & 1 & 0 & 0 & 0 \\
0 & 0 & 0 & 0 & 0 & 0 & 0 & 0 & 0 & 1 & 0 & 0 \\
0 & 0 & 0 & 0 & 0 & 0 & 0 & 0 & 0 & 0 & 1 & 0 \\
0 & 0 & 0 & 0 & 0 & 0 & 0 & 0 & 0 & 0 & 0 & 1
\end{array}\right)$$

3. 2D Bosonization

As with the 2D KW, we consider the square lattice with fermions initialized in the empty state on the A sublattice and spins are initialized in $|+\rangle$ state on the B sublattice. We will create an "SPT" state (see below for caveats) protected by fermion-parity symmetry and a global 1-form symmetry. The stabilizers of this "JW state" are given by

$$\begin{array}{c} | \\ Z \\ | \\ -Z-P-Z- \\ | \\ Z \\ | \end{array} \qquad \begin{array}{c} | \\ Z \\ | \\ i\gamma-X-\gamma' \end{array} \qquad \begin{array}{c} -Z-\gamma' \\ | \\ X \\ | \\ i\gamma \end{array} \tag{B7}$$

Like the 1D example in the main text, this SPT can be prepared using a circuit that hops fermions across edges conditional on the state of the spin at that edge. The only novel subtlety—not present in the bosonic case or the 1D JW–is that these gates do not mutually commute. Nevertheless, it turns out that their ordering is irrelevant: each choice of ordering gives a valid JW transformation (which are all related by CZ gates)[83, 84]; a given choice determines the spatial anisotropy of the stabilizers, as in Eq. (B7).

Upon measuring the fermion parity of all fermions, the resulting state is described by stabilizers

(B8)

which up to a sign given by measurement outcomes, describes the 2D toric code.

The JW state has the property that if we form the open string operator associated to the 1-form symmetry, by taking a product of stabilizers, we will find a fermion operator at the end. It thus looks like a non-trivial SPT for fermion parity and the 1-form symmetry. However, if we consult the cobordism classification, we find there are no non-trivial SPTs in this symmetry class. In fact if we try to construct an SPT class with this property using the Atiyah-Hirzebruch spectral sequence we find that the relevant class in $H^2(\mathbb{Z}_2[1], \Omega^1_{\text{spin}})$ has a non-zero differential. It would be a supercohomology class but it does not satisfy the Gu-Wen equation [107] (also see [155]).

The puzzle is resolved by considering the cobordism classification as describing a torsor rather than a group, meaning that with this choice of 1-form symmetry, the associated open string must always end on a fermion, and in that sense there is only one SPT phase, but it is not quite trivial because the 1-form symmetry generator we've chosen is not completely "on-site".

Indeed, in [111**?**] it was stressed that the 1-form symmetry in 2+1D bosonization has an anomaly Sq^2B (unlike in 1+1D bosonization where we get an anomaly-free $\mathbb{Z}_2$ symmetry upon bosonizing) and the kernel of the bosonization transformation gives a trivialization of this anomaly in the presence of fermions. Very simply, the Sq^2B anomaly says that the 1-form symmetry generator needs to obey fermionic statistics. Now, there is no issue with realizing such an anomalous symmetry in a not-on-site fashion, but because of the anomaly it cannot be screened—there is no end-point operator that will give the open string long-range order. However, if physical fermions are present, we can have a short-range entangled state where the 1-form symmetry generator ends on these fermions, and we interpret this as a trivialization of the Sq^2B anomaly. This is precisely what happens in the JW state. We see to trivialize the anomaly, the 1-form symmetry generator has to end on a fermion (this is essentially the Gu-Wen equation), and so while it looks like a nontrivial SPT, there is really only one option, in harmony with the classification.

Appendix C: Equality of long-range order for measurement outcomes in 1D

In Section V A 1 in the main text, we claimed that $\langle\psi_0|Z_{2m}Z_{2n}|\psi_0\rangle = -\langle\psi_1|Z_{2m}Z_{2n}|\psi_1\rangle$. This can be derived using the notion of symmetry fractionalization [24]. In particular, since we have a gapped phase with $\prod_k X_{2k}$ symmetry, one can argue that $X_{2p}X_{2p+2}\cdots X_{2q}|\psi\rangle = U_L U_R|\psi\rangle$, where $U_{L,R}$ are exponentially localized near the endpoints of the original string operator. Equivalently, if we define $\tilde{\mathcal{S}}_{2p,2q} = X_{2p}X_{2p+2}\cdots X_{2q}$, then our state $|\psi\rangle$ is an eigenstate of $U_L\tilde{\mathcal{S}}_{2p,2q}U_R$. Since we are in a non-trivial SPT phase, $U_{L,R}$ will anti-commute with the other $\mathbb{Z}_2$ symmetry $\prod_k X_{2k-1}$. Let us now revisit the situation studied in the main text, where n and m are separated far from one another. Then we can choose $m \ll p \ll n \ll q$ such that $\mathcal{S}_{2m,2n} \times U_L\tilde{\mathcal{S}}_{2p,2q}U_R = -U_L\tilde{\mathcal{S}}_{2p,2q}U_R \times \mathcal{S}_{2m,2n}$. Note that since this operator leaves $|\psi\rangle$ invariant and toggles $\mathcal{S}_{2m,2n}$, we have that $U_L\tilde{\mathcal{S}}_{2p,2q}U_R|\psi_0\rangle = e^{i\alpha}|\psi_1\rangle$. Thus:

$$\langle\psi_0|Z_{2m}Z_{2n}|\psi_0\rangle = e^{-i\alpha}\langle\psi_0|Z_{2m}Z_{2n}U_L\tilde{\mathcal{S}}_{2p,2q}U_R|\psi_1\rangle = -e^{-i\alpha}\langle\psi_0|U_L\tilde{\mathcal{S}}_{2p,2q}U_R Z_{2m}Z_{2n}|\psi_1\rangle = -\langle\psi_1|Z_{2m}Z_{2n}|\psi_1\rangle, \quad \text{(C1)}$$

where we used that Z_{2n} is odd under the spin-flip symmetry on the even sites, and since $m \ll p \ll n \ll q$ it is thus odd under $\tilde{\mathcal{S}}_{2p,2q}$ (whereas Z_{2m} is not).